

Smectite Clays as Solid Supports for Immobilization of β -Glucosidase: Synthesis, Characterization, and Biochemical Properties

Evangelia Serefoglou,[†] Kiriaki Litina,[†] Dimitrios Gournis,^{*,†,‡} Emmanuel Kalogeris,[§] Aikaterini A. Tziiala,[§] Ioannis V. Pavlidis,[§] Haralambos Stamatis,^{*,§} Enrico Maccallini,^{‡,||} Monika Lubomska,[‡] and Petra Rudolf^{*,‡}

Department of Materials Science and Engineering and Department of Biological Applications and Technologies, University of Ioannina, GR-45110 Ioannina, Greece, Zernike Institute for Advanced Materials, University of Groningen, Nijenborgh 4, NL 9747 AG, Groningen, The Netherlands, and Department of Physics, University of Calabria, via P. Bucci, I-87036 Arcavacata di Rende (Cs), Italy

Received February 19, 2008. Revised Manuscript Received April 15, 2008

Nanomaterials as solid supports can improve the efficiency of immobilized enzymes by reducing diffusional limitation as well as by increasing the surface area per mass unit and therefore improving enzyme loading. In this work, β -glucosidase from almonds was immobilized on two smectite nanoclays. The resulting hybrid biocatalysts were characterized by a combination of powder X-ray diffraction, X-ray photoelectron spectroscopy, thermogravimetric analysis, differential thermal analysis, and infrared spectroscopy. Biochemical studies showed an improved thermostability of the immobilized enzyme as well as enhanced performance at higher temperatures and in a wider pH range.

Introduction

β -D-Glucoside glucohydrolases (E.C. 3.2.1.21) or β -glucosidases constitute a group of well-characterized, biologically important enzymes that catalyze *in vivo* the cleavage of glycosidic bonds in oligosaccharides or glycoconjugates. Moreover, by reversing the normal hydrolytic reaction, β -glucosidases can potentially be used in the synthesis of glycosyl bonds between different molecules.^{1,2}

Glucosidases, due to their ability of bioconversion of lingocellulosic feedstocks to fuel grade ethanol, have found varied applications in biotechnology and food technology.³ The synthetic activity of β -glucosidases can be used in the preparation of a variety of compounds such as oligosaccharides and glycoconjugates that have potential for use as agrochemicals and drugs.⁴ Immobilized glucosidases are utilized in many large-scale processes, mainly because they allow for catalyst recycling, continuous operation, and controlled product formation. Adsorption via covalent binding to solid supports, entrapment in polymer hydrogels, and microencapsulation are common methods to immobilize glucosidases from different sources to various supports

including resins,¹ calcium alginate gels,⁵ agarose gels,⁶ silica gel,⁷ carbon nanotubes,⁸ and polymer carriers such as nylon^{9,10} and Eupergit C.¹¹ Obviously, the structural characteristics of the support are important since they may influence the catalytic behavior and stability of the immobilized enzyme.¹² Reduction of dimensions of enzyme-carrier materials can generally improve the catalytic efficiency of immobilized enzymes.^{8,13} Recently, the interest in nanomaterials and nanostructured materials as supports for enzyme immobilization has been growing^{13–15} since nanomaterials can enhance the efficiency of immobilized enzymes by reducing the diffusional limitation as well as by increasing the surface area per mass unit and therefore improving enzyme loading.¹³

Smectite clays are layered minerals, consisting of nanometer-sized aluminosilicate nanoplatelets, with a unique combination of swelling, intercalation, and ion exchange properties that make them valuable nanostructures in diverse

* Corresponding authors. E-mail: (D.G.) dgourni@cc.uoi.gr; (H.S.) hstamati@cc.uoi.gr; and (P.R.) p.rudolf@rug.nl.

[†] Department of Materials Science and Engineering, University of Ioannina.

[‡] University of Groningen.

[§] Department of Biological Applications and Technologies, University of Ioannina.

^{||} University of Calabria.

(1) Ducret, A.; Trani, M.; Lortie, R. *J. Mol. Catal. B: Enzym.* **2006**, *38*, 91.

(2) Yi, Q.; Sarney, D. B.; Khan, J. A.; Vulfson, E. N. *Biotechnol. Bioeng.* **1998**, *60*, 385.

(3) Bhatia, Y.; Mishra, S.; Bisaria, V. S. *Crit. Rev. Biotechnol.* **2002**, *22*, 375.

(4) Fischer, L.; Bromann, R.; Kengen, S. W. M.; de Vos, W. M.; Wagner, F. *Biotechnology* **1996**, *14*, 88.

(5) Busto, M. D.; Ortega, N.; Perez Mateos, M. *Process Biochem. (Oxford, U.K.)* **1997**, *32*, 441.

(6) Spagna, G.; Barbagallo, R. N.; Pifferi, P. G.; Blanco, R. M.; Guisan, J. M. *J. Mol. Catal. B: Enzym.* **2000**, *11*, 63.

(7) Synowiecki, J.; Wolosowska, S. *Enzyme Microb. Technol.* **2006**, *39*, 1417.

(8) Gomez, J. M.; Romero, M. D.; Fernandez, T. M. *Catal. Lett.* **2005**, *101*, 275.

(9) Woodward, J. R.; Radford, A.; Rodriguez, L.; Aguado, J.; Romero, M. D. *Acta Biotechnol.* **1992**, *12*, 357.

(10) Isgrove, F. H.; Williams, R. J. H.; Niven, G. W.; Andrews, A. T. *Enzyme Microb. Technol.* **2001**, *28*, 225.

(11) Tu, M. B.; Zhang, X.; Kurabi, A.; Gilkes, N.; Mabee, W.; Saddler, J. *Biotechnol. Lett.* **2006**, *28*, 151.

(12) Bornscheuer, U. T. *Angew. Chem., Int. Ed.* **2003**, *42*, 3336.

(13) Kim, J.; Grate, J. W.; Wang, P. *Chem. Eng. Sci.* **2006**, *61*, 1017.

(14) Jia, H. F.; Zhu, G. Y.; Wang, P. *Biotechnol. Bioeng.* **2003**, *84*, 406.

(15) Caruso, F.; Schuler, C. *Langmuir* **2000**, *16*, 9595.

fields.^{16–19} The intercalation process in these systems is equivalent to ion exchange and, unlike for intercalation compounds of graphite, it does not necessarily involve charge transfer between guest and host species. Smectite clays have a natural ability to adsorb organic and inorganic cationic species or even neutral guest molecules from solutions. Because of their unique properties, clay minerals can be used as catalysts,^{20,21} templates^{22,23} in organic synthesis, or as building blocks for composite materials.^{24–29} The nature of the microenvironment between the aluminosilicate sheets regulates the topology of the intercalated molecules and affects possible supramolecular rearrangements or reactions, such as self-assembling processes that are usually difficult to control in solution.^{24–31} Because of the high affinity of expandable clays for protein adsorption, the immobilization of enzymes on clay minerals has been studied during the last few decades.^{32–36} Globular proteins, such as enzymes, may be adsorbed on both the external and the internal surfaces of the layered aluminosilicate minerals.³³ The sorption ability of clays with regard to enzymes depends strongly on the pH and temperature of the immobilization reaction, the cation exchange capacity and surface area of the clay minerals, the nature of the interlayer exchangeable cations, the isoelectric point, as well as the size of the enzyme. Cellulase,³² aspartase,³⁵ albumin,³³ glucose oxidase,³⁴ catalase,³⁷ tyrosinase,³⁸ lipase,^{39,40} amylase,⁴¹ and glucoamylase³⁶ are examples of enzymes that have been immobilized on nonmodified and modified clays. In most

cases, adsorption occurs on the external surface of the layered clay; however, in few cases such as albumin,³³ glucose oxidase,³⁴ or aspartase,³⁵ partial intercalation was observed. Nevertheless, catalytic activity and biochemical characterization, such as pH profile and thermal stability, of the hybrid biocatalysts were not examined in detail in these studies.

In the present work, β -glucosidase from almonds was immobilized on two representative clays of the smectite group: a natural montmorillonite (kunipia) and a synthetic hectorite (laponite). Since these two clays have different structural and physical parameters, we examined the effect of platelet size and cation exchange capacity (CEC) on enzyme immobilization. The resulting new hybrid biocatalysts were characterized by a combination of analytical techniques such as powder X-ray diffraction (XRD), X-ray photoelectron spectroscopy (XPS), thermogravimetric analysis (TGA), differential thermal analysis (DTA), and infrared spectroscopy (FT-IR). Biochemical properties, namely, thermostability, pH and temperature profile, as well as enzyme kinetics, were explored and compared with the properties of free β -glucosidase. The availability and low cost of clays, their easy handling, improved thermostability of the enzyme, as well as remarkable performance of the enzyme at higher temperatures and in a wide pH range are some of the advantages of the present immobilization method.

Experimental Procedures

Enzyme and Reagents. β -Glucosidase from almonds was obtained from Sigma Chemicals in the form of lyophilized powder with a specific activity of 5.3 U per mg of protein (1 mg of powder is equal to 1 mg of protein) and stored at 4 °C. All chemicals used in the present study were of the highest purity commercially available.

Host Layered Materials. Two different clays were used in this work: a trioctahedral hectorite (laponite, LAP) obtained from Laporte Industries Ltd. with a particle size of 200 nm and CEC of 50 mequiv per 100 g of clay and a natural dioctahedral montmorillonite (kunipia, KUN) from Kunimine Industries Co. with a particle size of 2000 nm and CEC of 120 mequiv per 100 g of clay. The natural clay was fractionated to <2 μ m by gravity sedimentation and purified by standard clay science⁴² methods. Sodium-exchanged samples were prepared by immersing the clay into a 1 N solution of sodium chloride. Cation exchange was completed by washing and centrifuging 4 times with an aqueous solution of 1 N NaCl. The samples were finally washed with distilled deionized water, transferred into dialysis tubes to obtain chloride-free clays, and dried at room temperature.

Immobilization of β -Glucosidase in Layered Materials. In a typical synthetic procedure, 100 mg of the clay was dispersed in 5 mL of 100 mM acetate buffer (pH 5.0), and to this prepared suspension, 5 mL of aqueous enzyme (β -glucosidase) solution, buffered at the same pH, was added in different enzyme/clay ratios: 20, 50, 100 and 200 mg of lyophilized enzyme powder per 1 g of clay. The temperature during the reaction was kept below 5 °C, and the mixture was stirred overnight. The sample was then centrifuged, washed twice with the buffer solution, and air-dried by being spread on a glass plate at a temperature below 8 °C (products: LAP-R and KUN-R, where R = 20, 50, 100, or 200 mg of enzyme per 1 g of clay). The determination of the enzyme

- (16) Pinnavaia, T. J. *Science (Washington, DC, U.S.)* **1983**, 220, 365.
- (17) Konta, J. *Appl. Clay Sci.* **1995**, 10, 275.
- (18) Lagaly, G. *Solid State Ionics* **1986**, 22, 43.
- (19) Newman, A. C. D. *Chemistry of Clays and Clay Minerals; Mineralogical Society Monograph, No. 6*; Longman: London, 1987.
- (20) Ballantine, J. A. *NATO-ASI Ser., Ser. C* **1986**, 165, 197.
- (21) Cornelis, A.; Laszlo, P. *NATO-ASI Ser., Ser. C* **1986**, 165, 213.
- (22) Georgakilas, V.; Gournis, D.; Petridis, D. *Angew. Chem., Int. Ed.* **2001**, 40, 4286.
- (23) Georgakilas, V.; Gournis, D.; Bourlinos, A. B.; Karakassides, M. A.; Petridis, D. *Chem.—Eur. J.* **2003**, 9, 3904.
- (24) Theng, B. K. G. *The Chemistry of Clay Organic Reactions*; Adam Hilger: London, 1974.
- (25) Klopogge, J. T. J. *Porous Mater.* **1998**, 5, 5.
- (26) Gil, A.; Gandia, L. M.; Vicente, M. A. *Catal. Rev.—Sci. Eng.* **2000**, 42, 145.
- (27) Ma, Y.; Tong, W.; Zhou, H.; Suib, S. L. *Microporous Mesoporous Mater.* **2000**, 37, 243.
- (28) Ohtsuka, K. *Chem. Mater.* **1997**, 9, 2039.
- (29) Shichi, T.; Takagi, K. *J. Photochem. Photobiol., C* **2000**, 1, 113.
- (30) Gournis, D.; Georgakilas, V.; Karakassides, M. A.; Bakas, T.; Kordatos, K.; Prato, M.; Fanti, M.; Zerbetto, F. *J. Am. Chem. Soc.* **2004**, 126, 8561.
- (31) Gournis, D.; Jankovic, L.; Maccallini, E.; Benne, D.; Rudolf, P.; Colomer, J. F.; Sooambar, C.; Georgakilas, V.; Prato, M.; Fanti, M.; Zerbetto, F.; Sarova, G. H.; Guldi, D. M. *J. Am. Chem. Soc.* **2006**, 128, 6154.
- (32) Safari Sinegani, A. A.; Emtiaz, G.; Shariatmadari, H. *J. Colloid Interface Sci.* **2005**, 290, 39.
- (33) De Cristofaro, A.; Violante, A. *Appl. Clay Sci.* **2001**, 19, 59.
- (34) Garwood, G. A.; Mortland, M. M.; Pinnavaia, T. J. *J. Mol. Catal.* **1983**, 22, 153.
- (35) Naidja, A.; Huang, P. M. *J. Mol. Catal. A: Chem.* **1996**, 106, 255.
- (36) Gopinath, S.; Sugunan, S. *Appl. Clay Sci.* **2007**, 35, 67.
- (37) Fusi, P.; Ristori, G. G.; Calamai, L.; Stotzky, G. *Soil Biol. Biochem.* **1989**, 21, 911.
- (38) Naidja, A.; Huang, P. M.; Bollag, J. M. *J. Mol. Catal. A: Chem.* **1997**, 115, 305.
- (39) de Fuentes, I. E.; Viseras, C. A.; Ubiali, D.; Terreni, M.; Alcantara, A. R. *J. Mol. Catal. B: Enzym.* **2001**, 11, 657.
- (40) Secundo, F.; Miehe-Brendle, J.; Chelaru, C.; Ferrandi, E. E.; Dumitriu, E. *Microporous Mesoporous Mater.* **2008**, 109, 350.
- (41) Sanjay, G.; Sugunan, S. *Clay Miner.* **2005**, 40, 499.

- (42) King, R. D.; Nocera, D. G.; Pinnavaia, T. J. *J. Electroanal. Chem.* **1987**, 236, 43.

immobilized on clays was based on protein measurements in the liquid phase and washings obtained during the immobilization process, according to the dye-binding method of Bradford.⁴³

Enzyme Assay. The activity of β -glucosidase was determined spectrophotometrically following 10 min of incubation of the enzyme with 1 mM *p*-nitrophenyl- β -D-glucopyranoside (pNPG) in 100 mM citrate-phosphate buffer solution, pH 5.0.⁴⁴ The mixture was incubated at 37 °C in a rotary shaker, and the reaction was terminated by the addition of 30% (w/v) sodium carbonate solution. The solid particles, present after the immobilized form of the enzyme was assayed, were removed by centrifugation at 4000 rpm for 5 min. The increase in absorbance at 410 nm, due to *p*-nitrophenol release, was measured using a Hitachi 2000 UV–vis spectrophotometer. One unit (U) was defined as the amount of enzyme required to catalyze the formation of 1 μ mol of product during 1 min at the conditions described previously.

Powder XRD. The XRD patterns were collected on a D8 Avance Bruker diffractometer using Cu K α (40 kV, 40 mA) radiation and a secondary beam graphite monochromator. The patterns were recorded in a 2θ range from 2 to 30°, in steps of 0.02° and counting time of 2 s per step. Samples were in the form of films on a glass substrate.

FT-IR Spectroscopy. IR spectra were measured using a Shimadzu FT-IR 8400 spectrometer, equipped with a deuterated triglycine sulfate (DTGS) detector, in the region of 4000–400 cm^{-1} . Each spectrum was the average of 64 scans collected with 2 cm^{-1} resolution. Samples were in the form of KBr pellets containing ca. 2% (w/w) of the sample. The spectrum of the aqueous solution of β -glucosidase (100 mM acetate buffer, pH 5, 10 mg/mL protein concentration) was measured on a zinc selenide attenuated total reflectance (ATR) accessory. For this spectrum, a 64 scan interferogram was collected at a resolution of 2 cm^{-1} between 4000 and 400 cm^{-1} . To obtain the protein spectra in both pellets and aqueous solution, KBr and buffer spectra were subtracted by adjusting the subtraction factor until a flat baseline was obtained in the 2200–1800 cm^{-1} region.

FT-IR Data Analysis on Amide I Band. All spectra were smoothed with an 11 point Savitsky–Golay function to remove the possible noise before further data analysis of the amide I region. The data were manipulated using WinSpec software (LISE-Facultés Universitaires Notre-Dame de la Paix, Namur, Belgium). Band positions were identified from the second derivative spectra. The band positions obtained that way and a half-bandwidth of 11 cm^{-1} were used as the initial guess for Gaussian curve fitting. The deviation of the values for the half-bandwidth was from 10 to 13 cm^{-1} . The deviation for the position was limited to ± 2 cm^{-1} . Best curve-fitting was obtained at the lowest possible χ^2 values.

Thermal Analysis. TGA and DTA analyses were performed using a PerkinElmer Pyris Diamond TG/DTA instrument. Samples of approximately 5 mg were heated in air from 25 to 600 °C, at a rate of 5 °C/min.

XPS. Samples introduced through a load lock system were measured using a SSX-100 (Surface Science Instruments) photoelectron spectrometer with a monochromatic Al K α X-ray source ($h\nu = 1486.6$ eV). The base pressure in the spectrometer was 10^{-10} Torr, and the energy resolution was set to 1.16 eV to minimize measuring time. The photoelectron takeoff angle was set at 37°, and an electron flood gun was used to compensate for sample charging. Evaporated gold films on glass served as substrates. Clay/enzyme nanocomposites, as well as the free enzyme, were dispersed

in distilled deionized water, and after stirring and sonication for 10 min, a small drop of the suspension was deposited onto the substrate and left to dry in air. The binding energies of the clay/enzyme nanocomposites were referenced to the Si 2p binding energy of the clay silicon (102.8 eV),⁴⁵ while the binding energy of free β -glucosidase was referenced to the peak of C–C/C–H bonds in the C 1s spectrum of glucose oxidase at 285.0 eV.^{46–49} Glucose oxidase was chosen as a reference since, to the best of our knowledge, there are no XPS data on glucosidase itself in the literature and the local electronic structure of the two enzymes is nearly the same. Spectral analysis included a background subtraction (Shirley background) and peak separation using Gaussian functions, in a least-squares curve-fitting program (WinSpec).

Determination of Kinetic Constants. The initial rate of enzymic reaction as a function of *p*-NPG concentration was measured for both free and immobilized enzyme over the 0–20 mM range. Parametric identification of maximum velocity (V_{max}) and Michaelis–Menten constants (K_m) was used for initial reaction velocity. The program of identification was the Enzfitter software from the Biosoft Corp.

pH and Temperature Profile. The optimum temperature was determined by assaying the enzyme activity at various temperatures (30–75 °C) in 100 mM citrate-phosphate buffer solution (pH 5.0). The optimum pH was determined by measuring the activity at 37 °C over the pH range of 4.0–9.0 using 100 mM citrate-phosphate buffer.

Enzyme Stability. The stability of both free and immobilized β -glucosidase was assessed both at 55 and at 60 °C. Following incubation of enzyme suspensions in 100 mM citrate-phosphate buffer solution, pH 5.0, in a water bath with stirring for various time intervals, the residual enzyme activity was determined as described previously. The inactivation rate constants (k_d) of the enzyme were calculated through first-order inactivation kinetics.⁵⁰

Results and Discussion

The intercalation capability of the enzyme was evaluated by XRD measurements. A series of XRD patterns recorded from sodium-laponite (LAP) and hybrid systems LAP-20, LAP-50, LAP-100, and LAP-200 are shown in Figure 1A. An increase of the basal spacing (d_{001}) of the clay mineral was observed after sorption and immobilization of the enzyme. More specifically, the pristine sodium-laponite shows a d_{001} spacing of 12.8 Å, which corresponds to an intersheet separation $\Delta = 12.8 - 9.6 = 3.2$ Å, where 9.6 Å is the thickness of the clay layer,²⁴ while in the case of LAP-20 and LAP-50, the d_{001} spacing becomes 14.5 Å, pointing to an intersheet separation of $\Delta = 14.5 - 9.6 = 4.9$ Å. This 4.9 Å interlayer distance arises from a conformation where part of the enzyme enters into the intersheet space while the major part is located at the external surfaces and near the edge sites of laponite clay. This partial intercalation is in agreement with various literature data on the immobilization

(43) Bradford, M. M. *Anal. Biochem.* **1976**, *72*, 248.

(44) Kalogeris, E.; Christakopoulos, P.; Katapodis, P.; Alexiou, A.; Vlachou, S.; Kekos, D.; Macris, B. J. *Process Biochem. (Oxford, U.K.)* **2003**, *38*, 1099.

(45) Ebina, T.; Iwasaki, T.; Chatterjee, A.; Katagiri, M.; Stucky, G. D. *J. Phys. Chem. B* **1997**, *101*, 1125.

(46) Curulli, A.; Cusma, A.; Kaciulis, S.; Padeletti, G.; Pandolfi, L.; Valentini, F.; Viticoli, M. *Surf. Interface Anal.* **2006**, *38*, 478.

(47) De Benedetto, G. E.; Malitesta, C.; Zambonin, C. G. *J. Chem. Soc., Faraday Trans.* **1994**, *90*, 1495.

(48) Griffith, A.; Glidle, A.; Beamson, G.; Cooper, J. M. *J. Phys. Chem. B* **1997**, *101*, 2092.

(49) Griffith, A.; Glidle, A.; Cooper, J. M. *Biosens. Bioelectron.* **1996**, *11*, 625.

(50) Aymard, C.; Belarbi, A. *Enzyme Microb. Technol.* **2000**, *27*, 612.

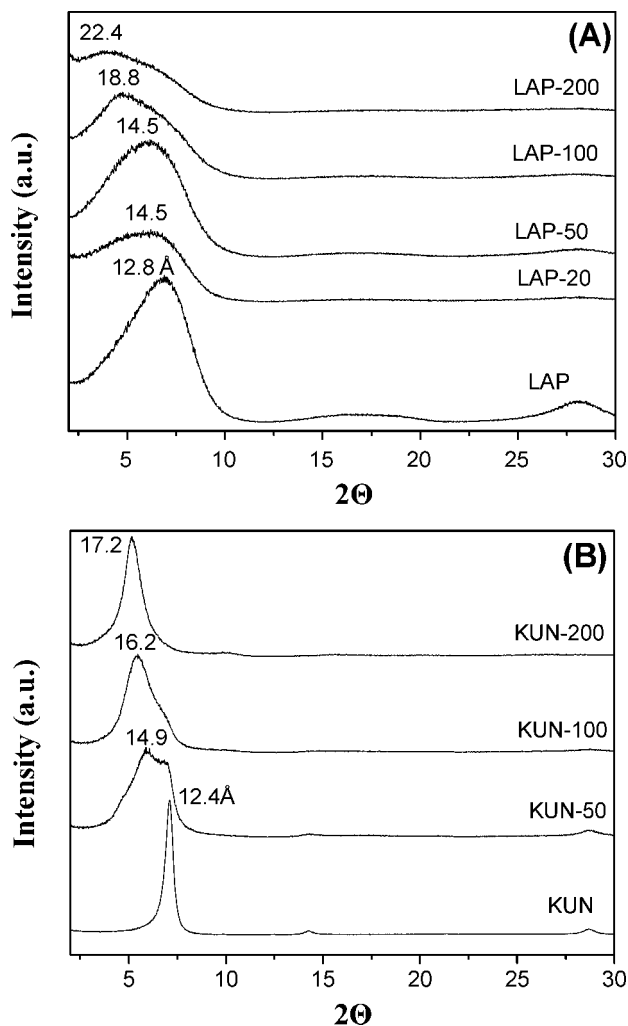


Figure 1. XRD patterns of (A) laponite composites (LAP, LAP-20, LAP-50, LAP-100, and LAP-200) and (B) kunipia composites (KUN, KUN-50, KUN-100, and KUN-200).

of enzymes in smectite clays; see, for example, reports for cellulase,³² aspartase,³⁵ albumin,³³ or glucose oxidase.³⁴ After the addition of 100 mg of enzyme per 1 g of clay, the d_{001} spacing increased to 18.8 Å ($\Delta = 9.2$ Å), indicating that a larger portion of the enzyme was inserted in the clay galleries. Finally, at a maximum loading of 200 mg per 1 g of clay, the (001) diffraction peak appeared at a higher spacing of 22.4 Å, confirming the remarkable binding capacity of laponite clay for β -glucosidase. Since the d_{001} spacing of the clay without intercalant is 9.6 Å, the lattice expansion due to intercalated enzyme is ~ 12.8 Å. However, this value is much smaller than the expected size (50–60 Å) of the small active component of β -glucosidase from almonds (i.e., globular protein with a molecular weight of 66.5 kDa).^{51,52} Even if the enzyme shape is likely to be more oblate in the intercalated state than in homogeneous solution,³⁴ the present data reveal that a large part, but not all, of the enzyme is located in the interlamellar spacing. In fact,

(51) Helferich, B.; Kleinschmidt, T. *Hoppe-Seyler's Z. Physiol. Chem.* **1965**, *340*, 31.

(52) Grover, A. K.; Macmurchie, D. D.; Cushley, R. J. *Biochim. Biophys. Acta* **1977**, *482*, 98.

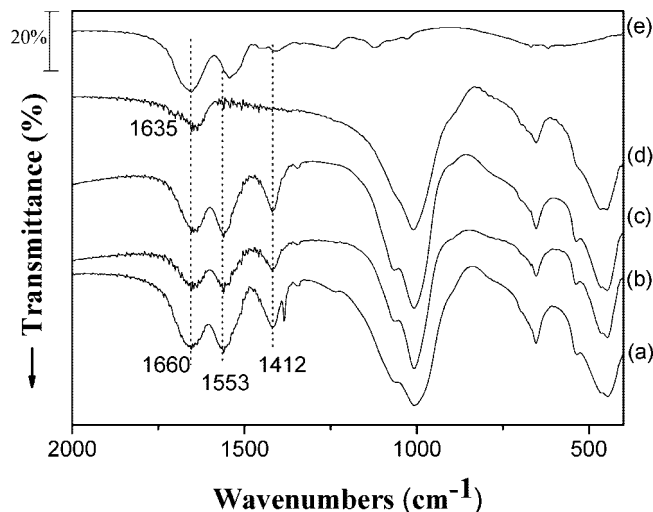


Figure 2. FT-IR spectra of (a) LAP-200, (b) LAP-100, and (c) LAP-50, (d) LAP, and (e) free β -glucosidase.

earlier studies by Morgan and Corke⁵³ showed that the maximum amount of glucose oxidase that could be bound in Na^+ -montmorillonite is 1 g of enzyme per 1 g of clay. At this maximum loading, a d spacing of 44 Å was observed by Garwood et al.,³⁴ due to fully intercalated complexes. Similar results were observed for montmorillonite: Figure 1B shows the XRD patterns of sodium-montmorillonite (KUN) and the hybrid systems containing various amounts of bound enzyme. The parent clay shows a main diffraction peak that corresponds to a d_{001} spacing of 12.4 Å. After the addition of 50 mg of enzyme (KUN-50), the clay exhibits a broad peak consisting of a 12.4 Å reflection typical of air-dried clay and a new reflection at 14.9 Å. As the amount of bound enzyme increases, the 12.6 Å line decreases in intensity, and the new diffraction peak appears at higher spacing (16.2 Å). We interpret this as being due to a larger segment of the enzyme entering into the interlayer space. The addition of 200 mg of enzyme per 1 g of clay gave a d_{001} spacing of 17.2 Å. This value is significantly lower than the one for laponite clay, probably because of the larger particle size of montmorillonite (2000 nm) as compared to laponite (200 nm). The small size of clay platelets in the case of laponite favors the insertion of segments of the huge enzyme, while the large size of montmorillonite platelets does not. Thus, in the case of montmorillonite, the binding of β -glucosidase takes place mainly in the external surface and at the edge sites of the clay mineral, while only a small part of the enzyme enters the interlamellar space.

Figure 2 shows the FT-IR spectra of the parent materials, sodium-laponite (LAP) and enzyme (β -glucosidase), and of the hybrid systems LAP-50, LAP-100, and LAP-200. The spectra of the composites present all the characteristic bands of laponite and β -glucosidase, without significant changes. More specifically, the appearance of the peaks at 448 and 1010 cm^{-1} , corresponding to Si–O and Si–O–Si vibrations of the clay lattice, indicates that the phyllosilicate mineral is present in the final composites. The peaks at 1660, 1553, and 1412 cm^{-1} in the spectra of the hybrid systems originate

(53) Morgan, H. W.; Corke, C. T. *Can. J. Microbiol.* **1976**, *22*, 684.

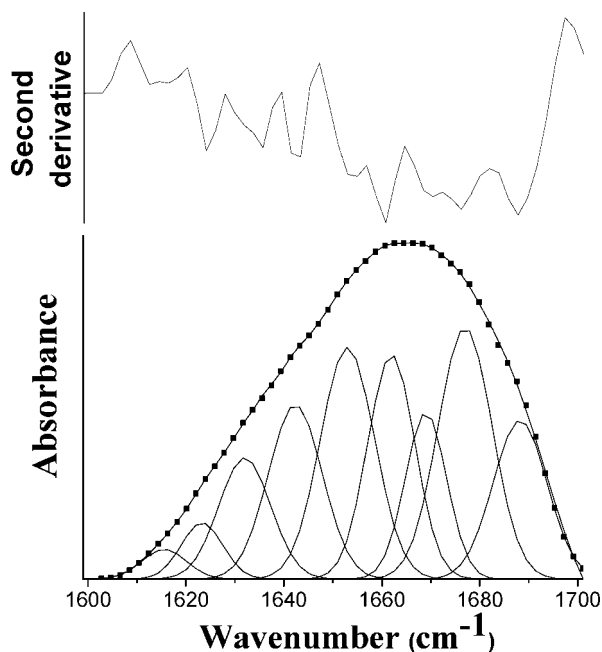


Figure 3. Second derivative and deconvoluted amide I spectra of β -glucosidase immobilized on kunipia montmorillonite (KUN-200).

from the enzyme and correspond to amide vibrations of the peptide group. In particular, the bands at 1660 and 1553 cm^{-1} , called amide I and amide II bands, are the two major bands of the protein infrared spectra.⁵⁴ The amide I band is mainly associated with the C=O stretching vibration and superimposed on it at 1635 cm^{-1} is the peak due to water deformation of the clay mineral, leading to a broader band. The amide II band results from the N-H vibration and from the C-N stretching vibration. Finally, the peak at 1412 cm^{-1} (amide III) depends on the nature of the side chains of the enzyme.⁵⁴ Similar spectra were observed for the sodium-montmorillonite hybrids (data not shown here). The spectra of the composites present characteristic peaks of kunipia (467 and 1039 cm^{-1}) plus those of β -glucosidase (1660, 1553, and 1412 cm^{-1}).

To obtain quantitative information about the protein secondary structure upon immobilization on smectite clays, a curve-fitting analysis of the amide I absorption band was performed for the spectra of hybrid biocatalysts, as a linear combination of the components identified in the second-derivative spectra. A representative spectrum (KUN-200) and the outcome of the fitting are depicted in Figure 3. The band assignment in the amide I region was based on similar studies reported in the literature for other proteins.^{55,56} The bands at 1620–1640 cm^{-1} can be assigned to β -sheets, at 1640–1650 cm^{-1} to random coils, at 1650–1660 cm^{-1} to α -helices, and at 1660–1685 cm^{-1} to β -turns, while the bands at 1610–1620 and 1685–1695 cm^{-1} are related to antiparallel β -sheets, mostly introduced in protein aggregates. Table 1 reports the secondary structure elements of β -glucosidase in aqueous solution and of the immobilized enzyme

Table 1. Estimation of Secondary Structure Elements (%) of β -Glucosidase by FT-IR Analysis in Amide I Region

sample	α -helix	β -sheet	β -turns	random coil
aqueous enzyme solution	28.4	29.3	30.2	12.1
KUN-100	17.3	26.7	44.2	11.9
KUN-200	17.5	25.9	43.4	13.2
LAP-100	16.9	27.6	44.4	11.1
LAP-200	17.5	23.3	46.0	13.1

on two different clays (laponite and montmorillonite) loaded with 100 and 200 mg of protein/g of clay. The enzyme secondary structure shows the same features in both supports, despite the difference in enzyme loading. The native structure of the enzyme in aqueous solution is modified upon immobilization on clays. There is a substantial decrease of the α -helix element and a lower percentage of the β -sheet form. The percentage of β -turns increased, but the random coil did not. This indicates that the immobilized enzyme retains an ordered structure, which is different from its native conformation, but catalytically active, as shown in biochemical results. Similar structural changes were observed in previous studies after the immobilization of enzymes on various supports.^{55,57}

Figure 4 shows the DTA-TGA curve, obtained in air, of the composite LAP-200, with higher loading, in comparison to those of pure enzyme and laponite clay, measured separately. Laponite clay displayed a 12% weight loss until 150 $^{\circ}\text{C}$ (endothermic), which is related to the evaporation of adsorbed water. On the other hand, pure β -glucosidase showed an $\sim 5\%$ weight loss until 100 $^{\circ}\text{C}$, and 95% between 200 and 550 $^{\circ}\text{C}$, with the exothermic peak centered at 340 $^{\circ}\text{C}$, due to oxidation of the protein molecule. Similar analysis of the LAP-200 composite demonstrated that the immobilized enzyme was 17% of the total mass. The DTA analysis of LAP-200 shows that the exothermal reactions of the oxidation of the enzyme are more defined as compared to those of the pure enzyme. More specifically, the main exothermic peak occurs at a similar temperature as before (330 $^{\circ}\text{C}$), whereas a new exothermic peak arises at a higher temperature (400 $^{\circ}\text{C}$) as compared to pure enzyme. The latter is probably due to the intercalated portion of the enzyme that is protected from the surroundings by aluminosilicate layers and thus oxidized at higher temperatures. From the weight loss curve, we roughly estimated that $\sim 40\%$ of the total amount of β -glucosidase was intercalated into the smectite clay. Analogous results were obtained for the montmorillonite/enzyme hybrid systems (data not shown here). In the case of the sample with the maximum loading, KUN-200, the amount of β -glucosidase corresponded to $\sim 12\text{ wt } \%$ of the total mass. The intercalated fraction was found to be $\sim 20\%$ of the total amount of enzyme. Both the total amount of β -glucosidase and the intercalated fraction are remarkably lower than in laponite composites, in agreement with XRD findings.

The starting materials (free enzyme, KUN, and LAP) and the produced nanocomposites were studied using XPS. XPS is a direct method to investigate as to how β -glucosidase binds to the siloxane interface and gives quantitative information on the elemental composition of hybrid systems.

(54) Venyaminov, S. Y.; Kalnin, N. N. *Biopolymers* **1990**, *30*, 1243.

(55) Fu, K.; Griebenow, K.; Hsieh, L.; Klibanov, A. M.; Langer, R. J. *Controlled Release* **1999**, *58*, 357.

(56) Kreilgaard, L.; Frokjaer, S.; Flink, J. M.; Randolph, T. W.; Carpenter, J. F. *J. Pharm. Sci.* **1999**, *88*, 281.

(57) Servagent-Noinville, S.; Revault, M.; Quiquampoix, H.; Baron, M. H. *J. Colloid Interface Sci.* **2000**, *221*, 273.

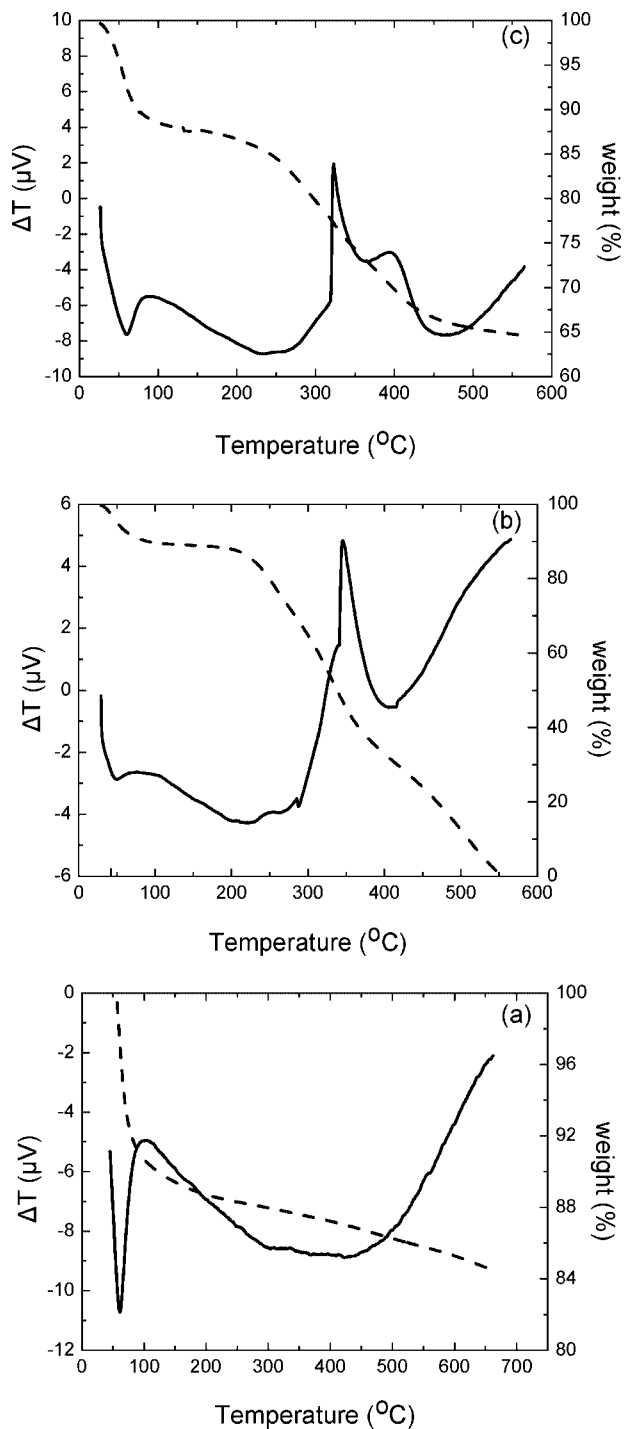


Figure 4. Thermogravimetric (dashed lines) and differential thermal (solid lines) curves of (a) Na^+ -laponite, (b) free β -glucosidase, and (c) LAP-200 composite.

While rigorously there are many chemically distinct carbon environments in enzymes, in practice, XPS may distinguish, for example, between aliphatic and carbonyl carbons but not between different types of carbonyls present in the molecule. Hence, the mathematical decomposition procedure consists of fitting a minimum number of peaks consistent with the raw data and the molecular structure. Figure 5 shows the C 1s core level emission spectra of free β -glucosidase and of the KUN-50 hybrid. For the former (Figure 5a), the experimental data were fitted (constrained by the theoretical intensity ratio) assuming a molecule with three distinct

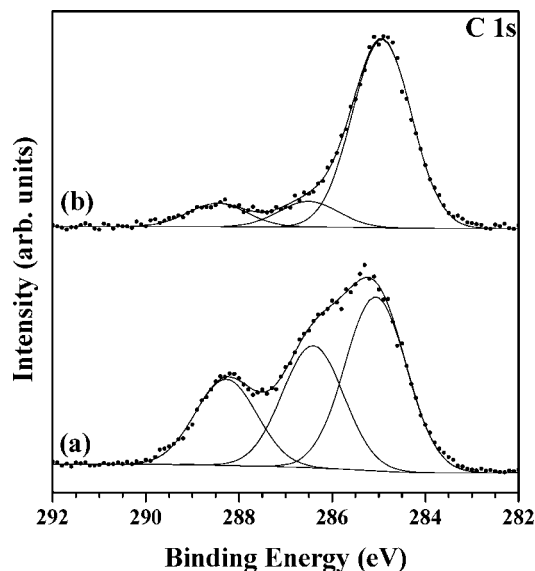


Figure 5. XPS spectra and fit of C 1s core level region for (a) free β -glucosidase and (b) KUN-50 nanocomposite.

chemically shifted C 1s core level emissions occurring at 285.0, 286.5, and 288.4 eV. The peak at 285.0 eV (C1) is assigned to C–C/C–H bonds of the aliphatic carbon. The peak at 286.5 eV (C2) is due to C–N/C–O bonds, while the peak at 288.4 eV (C3) arises from C=O bonds, both derived from the characteristic amide groups. These values are in agreement with those reported in the literature for glucose oxidase.^{46–49,58} The presence of amide groups also was established by analysis of binding energies of N 1s ($E_B = 400.1$ eV). The same peaks also were observed in the KUN-50 nanocomposite (Figure 5b), indicating that the immobilization of β -glucosidase on and in the clay does not cause any change in the electronic and chemical properties of the protein molecule. However, the relative intensities of the three C1s components are quite different from those of the free enzyme. In fact, in the KUN-50 hybrid, the spectral intensity of the C1 species seems to be increased with respect to that of the C2 and C3 species. This phenomenon indicates that the functional groups containing the C2 and C3 carbons are no longer located at the extreme surface of the sample, which causes their photoemission signal to be attenuated with respect to the free enzyme spectra. We can put forward the following explanation: The amide groups of β -glucosidase must be located close to the siloxane surface of the clay, similar to what was observed after the immobilization of glucose oxidase or horseradish peroxidase enzymes on TiO_2 and TiO_2/Si substrates,⁴⁶ and/or a selective intercalation of part of the amide groups in the clay interlayers has taken place, while comparatively more aliphatic groups of the enzyme are located outside of the lamellar space of the clay mineral.

Figure 6 (left) shows the C 1s core level emission spectra of hybrid systems containing various amounts of bound enzyme, namely, (a) KUN-50, (b) KUN-200, (c) LAP-50, and (d) LAP-200. When we compare the C 1s spectra of

(58) Viticoli, A.; Curulli, A.; Cusma, A.; Kaciulis, S.; Nunziante, S.; Pandolfi, L.; Valentini, F.; Padeletti, G. *Mater. Sci. Eng., C* **2006**, *26*, 947.

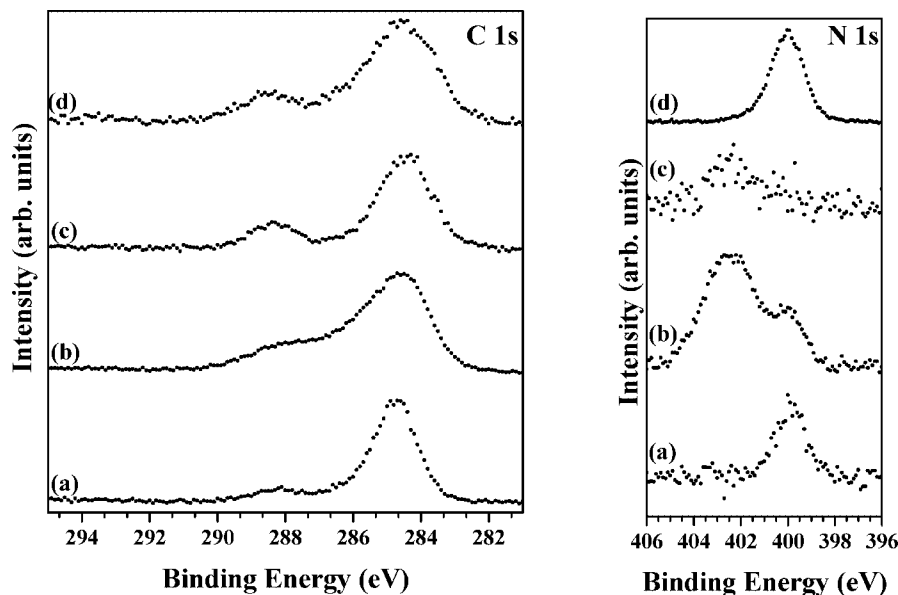


Figure 6. XPS spectra of the C 1s core level region (left) for (a) KUN-50, (b) KUN-200, (c) LAP-50, and (d) LAP-200 nanocomposites and N 1s core level region (right) for (a) KUN-50, (b) KUN-200, and (c) LAP-200 nanocomposites and (d) free β -glucosidase.

laponite/enzyme hybrids with low (a) and high (b) enzyme loading as well as the spectra with low (c) and high (b) loadings of LAP/enzyme hybrids, an enlargement of the width of the peaks is observed as the amount of intercalated enzyme increases (the fwhm of the peaks in the fit of C1s spectra (a–d) in Figure 6 (left) are 1.5, 1.9, 1.8, and 2.1 eV, respectively). This broadening is probably due to partial intercalation of the enzyme macromolecule in the clay interlayers and is in agreement with XRD findings. Clay platelets can cause screening of the C 1s core hole of C atoms in the intercalated segment of the enzyme, and this will result in broadening of the peaks because a screened core hole corresponds to a component at a slightly shifted binding energy. For larger amounts of bound enzyme, a larger portion of the enzyme enters the lamellar space, and hence, more C atoms will appear at different binding energies, giving rise to broader peaks. This interpretation is supported by the fact that the C 1s spectrum of LAP-200 is broader as compared to KUN nanocomposites, and its XRD results show that this sample has a higher d spacing after intercalation of β -glucosidase.

A similar analysis was performed for the N 1s spectra. In Figure 6 (right), we present the N 1s core level emission spectra of β -glucosidase and the KUN-50 and KUN-200 nanocomposites. While the spectra for the free enzyme (Figure 6 right, curve d) and for KUN-50 (curve a) show only one component at 400.1 eV due to the amide group of β -glucosidase, we observe an additional peak at higher (402.5 eV) binding energies for KUN-200 sample (curve b). This extra peak could be due to a different screening of the core hole when the amide group is further away from the clay surface. Such final state effects are usually observed at interfaces, a prominent example being the binding energy shifts observed in Xe multilayers⁵⁹ and expected to be particularly pronounced when there is a strong interface

Table 2. Effect of Enzyme/Carrier Mass Ratio on p -Nitrophenyl- β -D-glucopyranoside Hydrolysis Catalyzed by β -Glucosidase Immobilized on Clays

enzyme/carrier mass ratio	immobilization yield (%)		reaction rate ($\mu\text{mol min}^{-1} \text{g}^{-1}$ of biocatalyst)	
	laponite	kunipia	laponite	kunipia
0.02	91	85	0.50 ± 0.17	n.d. ^a
0.05	88	82	1.48 ± 0.33	1.45 ± 0.10
0.10	85	78	1.69 ± 0.23	1.85 ± 0.06
0.20	79	70	4.08 ± 0.36	2.30 ± 0.37

^a n.d.: not determined.

dipole such as at the clay/enzyme interface.⁶⁰ One can rationalize this observation by comparison with XRD data, which do not indicate a dramatic increase in intercalation upon going from KUN-50 to KUN-200 as in the case of LAP; therefore, for KUN-200, a larger amount of enzyme might be located on top of the first enzyme layer on the clay surface and not all amide groups are screened by electrostatic interactions at the surface. In the case of the LAP samples, the N 1s signal is extremely weak and even in the case of LAP-200 barely visible (Figure 6 right, curve c). This agrees with what we know from the diffraction data discussed previously, namely, that intercalation is much more important as compared to KUN. In fact, the intensity of intercalated amide groups will be even weaker than for those on the surface since the photoelectrons have to cross more material and are therefore more heavily attenuated. The higher binding energy N 1s component for LAP-200 is due to amide groups not in intimate contact with the clay surface.

The results concerning the activity of immobilized biocatalysts, obtained by varying the β -glucosidase/clay mass ratio during the immobilization process, are presented in Table 2. For all the protein concentrations examined, the implementation of the immobilization procedure created active biocatalysts for both clays. High proportions of initial enzyme loads (85% for hectorite and 78% for montmoril-

(59) Kaindl, G.; Chiang, T. C.; Eastman, D. E.; Himpsel, F. J. *Phys. Rev. Lett.* **1980**, *45*, 1808.

(60) Knupfer, M.; Peisert, H. *Phys. Status Solidi A* **2004**, *201*, 1055.

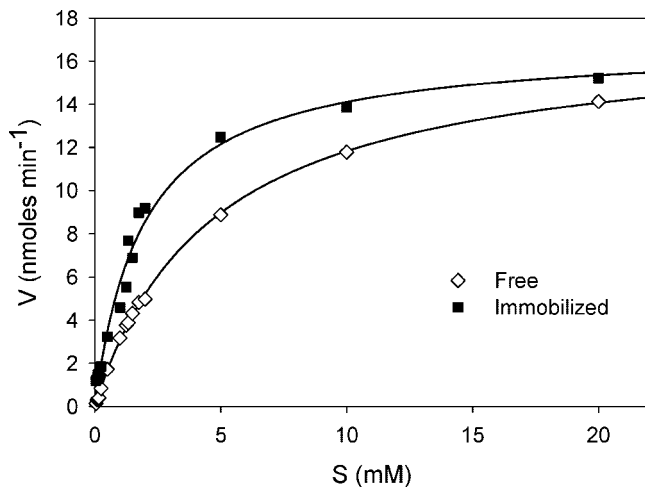


Figure 7. Michaelis–Menten plot of free and immobilized β -glucosidase.

lonite on average) remained attached on smectite particles following the immobilization process. Generally, the immobilization of enzymes (including β -glucosidase from almonds) on clays leads to high immobilization yields,⁶¹ in contrast to what was reported for other supports such as alumina,⁶² polymers,¹¹ gelatin,⁶³ silica,⁶⁴ etc., which gave low immobilization yields. When the enzyme/carrier mass ratio increased, higher reaction rates were observed, which indicates that, under the specific conditions applied in the present study, the saturation level of the clay was not reached. The enormous binding capacity of laponite was reconfirmed during the immobilization of glucose oxidase, where the application of much higher enzyme/carrier ratios (1.1–3.3) resulted in an almost complete entrapment of protein.⁶⁵ The highest reaction velocity of immobilized β -glucosidase was connected to the trioctahedral hectorite (laponite) at the highest protein concentration applied (0.2 g/g of clay), and the biocatalyst prepared under these conditions was used for further biochemical characterization experiments.

The Michaelis–Menten plots for free and immobilized enzyme are presented in Figure 7. The estimated values and standard errors of the Michaelis–Menten constant (K_m) for free and immobilized β -glucosidase for *p*-NPG hydrolysis were 4.7 ± 0.1 and 1.9 ± 0.2 mM, respectively. The turnover number that was estimated for immobilized enzyme ($154.1 \pm 5.1 \text{ min}^{-1}$) was very close to the corresponding value obtained for free enzyme ($159.6 \pm 1.8 \text{ min}^{-1}$). This is in agreement with previous findings where β -glucosidase immobilized on sandy alumina⁶² appeared to have a slightly lower reaction velocity (V_{max}) than the free enzyme. On the contrary, the immobilization process had a profound effect on enzyme affinity toward the substrate. This is in accordance with previous results, where the K_m value of immobilized

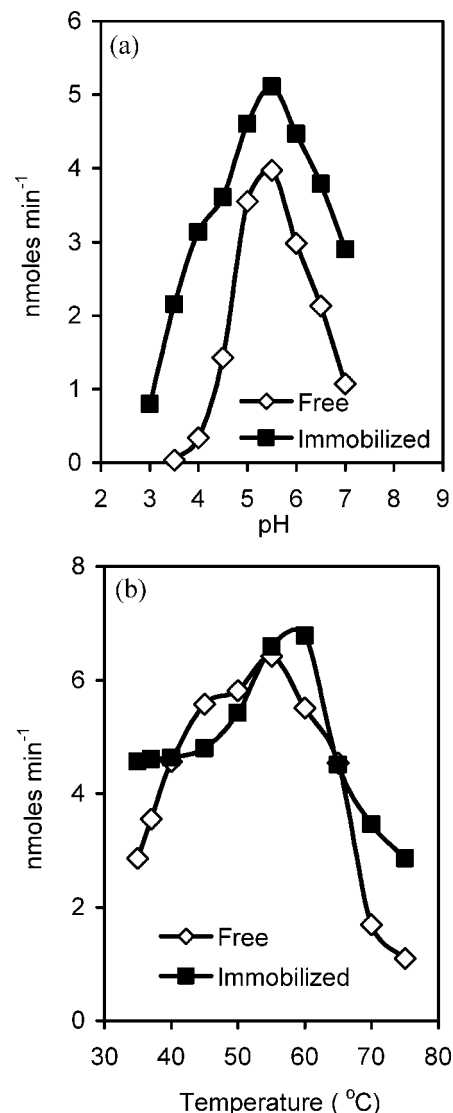


Figure 8. Effect of pH (a) and temperature (b) on free and immobilized β -glucosidase activity.

enzymes was lower than the corresponding value for free enzymes when ionic clays were used as host materials.⁶⁶ Moreover, the low K_m values associated with hosted enzymes have been considered to be an indication that clay templates provide a microenvironment around enzyme molecules without steric constraints.⁶⁷ The reduced K_m value, which was calculated for the immobilized enzyme in the present work, is indicative of stronger binding of substrate to enzyme molecules as well as negligible mass transfer limitations.⁶⁸ This could be, at least in part, a result of electrostatic interactions between the polar *p*-nitrophenyl moiety of the *p*-NPG molecule and the ionic environment created by the phyllosilicate carrier at the enzyme vicinity.

The effect of pH on the activity of both free and immobilized β -glucosidase is presented in Figure 8a. Although the optimum pH value (pH 5.5) was practically the same for the immobilized enzyme and free β -glucosidase,

(61) Sarkar, J. M.; Leonowicz, A.; Bollag, J. M. *Soil Biol. Biochem.* **1989**, *21*, 223.

(62) Fadda, M. B.; Dessi, M. R.; Rinaldi, A.; Satta, G. *Biotechnol. Bioeng.* **1989**, *33*, 777.

(63) Nagatomo, H.; Matsushita, Y.; Sugamoto, K.; Matsui, T. *Biosci. Biotechnol. Biochem.* **2005**, *69*, 128.

(64) O'Neill, H.; Angley, C. V.; Hemery, I.; Evans, B. R.; Dai, S.; Woodward, J. *Biotechnol. Lett.* **2002**, *24*, 783.

(65) Poyard, S.; Jaffrezic-Renault, N.; Martelet, C.; Cosnier, S.; Labbe, P. *Anal. Chim. Acta* **1998**, *364*, 165.

(66) Barhoumi, H.; Maaref, A.; Rammah, A.; Martelet, C.; Jaffrezic, N.; Mousty, C.; Vial, S.; Forano, C. *Mater. Sci. Eng., C* **2006**, *26*, 328.

(67) Da Silva, S.; Shan, D.; Cosnier, S. *Sens. Actuators, B* **2004**, *103*, 397.

(68) Trevan, M. *Trends Biotechnol.* **1987**, *5*, 7.

Table 3. Values (min^{-1}) of Deactivation Constant (k_d) for Free and Immobilized β -Glucosidase

temp ($^{\circ}\text{C}$)	free enzyme	immobilized enzyme
55	0.017 ± 0.002	0.011 ± 0.002
65	0.047 ± 0.009	0.026 ± 0.005

with initial reaction rates of 5.11 and 3.97 nmol min^{-1} , respectively, the immobilized enzyme displayed higher activities for pH values around the optimum. More specifically, the relative activity of the immobilized β -glucosidase at pH 3.5 and 7.0 was 42.1 and 56.8%, respectively, while the corresponding values for free enzyme were 1.1 and 27%, respectively. The different behavior of the two enzyme forms, in terms of pH variation, is evident from the comparison of the much broader bell-shaped curve of the immobilized enzyme with the curve obtained for free enzyme. Modified pH profile curves with either sharper or broader shapes have been reported as a consequence of enzyme immobilization.^{69–71}

In addition to variations in the pH profile, significant modifications in the temperature profile were observed after immobilization of the enzyme on laponite. The temperature profiles for both free and immobilized β -glucosidase are depicted in Figure 8b. The optimum temperature for the free enzyme was at 55 $^{\circ}\text{C}$, with an initial reaction rate of 6.42 nmol min^{-1} , while for immobilized β -glucosidase was at 60 $^{\circ}\text{C}$, with an initial reaction rate of 6.78 nmol min^{-1} . The pattern of the curve obtained for the immobilized enzyme was quite different from that obtained for the free enzyme. The performance of the enzyme at higher temperatures was substantially improved after immobilization: the relative activities of immobilized β -glucosidase at 70 and 75 $^{\circ}\text{C}$ were 51.0 and 42.2%, respectively, while the corresponding values for free enzyme were 26.3 and 17.0%, respectively. It is interesting that this improvement in enzyme performance was not observed for other supports, such as, for example, gelatin gel⁵⁹ used for the immobilization of this enzyme. An important difference between the two enzyme forms was the higher optimum temperature observed for the immobilized enzyme (~ 60 $^{\circ}\text{C}$) as compared to the corresponding value for free enzyme (~ 55 $^{\circ}\text{C}$), which is in agreement with previous findings, where the immobilized β -glucosidase on Eupergit C⁷¹ showed a maximum activity at 60 $^{\circ}\text{C}$, while the free form was most active around 50–55 $^{\circ}\text{C}$ under the same assay conditions.

In addition to altered pH profiles and improved activity at higher temperatures, immobilized enzymes usually exhibit an enhanced thermal stability.⁷² The deactivation constants (k_d) of free and immobilized β -glucosidase, for the two temperatures examined in the present study, are presented in Table 3. As can be seen, the k_d values for laponite-conjugated β -glucosidase are lower than the corresponding values estimated for the free enzyme; the difference was more prominent when the enzyme performance was investigated

at higher temperatures (65 $^{\circ}\text{C}$). Furthermore, the enzyme retained 61.8% of its activity, when immobilized on laponite and stored at 4 $^{\circ}\text{C}$ for 2 months, while the corresponding value for kunipia after 4 months of incubation was 66.5%. The results compare favorably with storage stability data for β -glucosidase in solution (more than 85% loss of enzyme activity after 2 months at 4 $^{\circ}\text{C}$)⁷³ and indicate that immobilization on clays could be an efficient method to improve the biochemical properties of enzymes. This is in agreement with previous work suggesting that mesoporous aluminosilicate materials⁷⁴ and clay minerals⁶¹ can be used as matrices for improving enzyme stability.

It is generally accepted that ionic interactions play a decisive role in thermostabilizing enzymes. Comparison of 13 structural parameters between 93 proteins from mesophilic and thermophilic microorganisms revealed that the only reliable rule was the increased number of ion pairs with increasing growth temperature, verifying the importance of electrostatic interactions in both moderately and extremely thermophilic proteins.⁷⁵ An increasing body of experimental evidence shows that ion pairs, especially networks of ion pairs, contribute to the increased thermal stability of several thermophilic proteins^{76–78} or even play a key role in thermostability.^{79–82} Accordingly, the improved enzyme thermostability observed in the present study, after immobilization on clays, could be attributed to the stabilizing effect of electrostatic interactions between the charged protein residues and the oppositely charged phyllosilicate layers.

Conclusion

The present results clearly demonstrate that smectite nanoclays can act as efficient supports for β -glucosidase immobilization. Two smectite clays, montmorillonite and laponite, with different structural and physical parameters were used to study the effect of platelet size and CEC on enzyme immobilization. The experimental results revealed that a significant portion, but not all, of the enzyme is located in the interlamellar spacing of the two smectites. The small size of the clay platelets in the case of laponite (200 nm) favored the insertion of segments of the huge enzyme, while the large platelet size of montmorillonite did not. Thus, in the case of montmorillonite, the binding of β -glucosidase takes place mainly in the external surface and at the edge sites of the clay mineral, and only a small portion of the enzyme enters the interlamellar space. The secondary

(69) Park, D.; Haam, S.; Jang, K.; Ahn, U. I.; Kim, W. S. *Process Biochem. (Oxford, U.K.)* **2005**, *40*, 53.

(70) Busto, M. D. *Biochem. Educ.* **1998**, *26*, 304.

(71) Fischer, L.; Peiker, F. *Appl. Microbiol. Biotechnol.* **1998**, *49*, 129.

(72) Novick, S. J.; Rozzell, J. D. *Immobilization of Enzymes by Covalent Attachment in Microbial Enzymes and Biotransformations*; J. L. Baredo Humana Press: Totowa, NJ, 2005.

(73) Chang, M. Y.; Juang, R. S. *Biochem. Eng. J.* **2007**, *35*, 93.

(74) Lee, C. H.; Lang, J.; Yen, C. W.; Shih, P. C.; Lin, T. S.; Mou, C. Y. *J. Phys. Chem. B* **2005**, *109*, 12277.

(75) Szilagy, A.; Zavodszky, P. *Structure* **2000**, *8*, 493.

(76) Chan, M. K.; Mukund, S.; Kletzin, A.; Adams, M. W. W.; Rees, D. C. *Science (Washington, DC, U.S.)* **1995**, *267*, 1463.

(77) Korndorfer, I.; Steipe, B.; Huber, R.; Tomschy, A.; Jaenicke, R. *J. Mol. Biol.* **1995**, *246*, 511.

(78) Kelly, C. A.; Nishiyama, M.; Ohnishi, Y.; Beppu, T.; Birktoft, J. J. *Biochemistry* **1993**, *32*, 3913.

(79) Aguilar, C. F.; Sanderson, I.; Moracci, M.; Ciaramella, M.; Nucci, R.; Rossi, M.; Pearl, L. H. *J. Mol. Biol.* **1997**, *271*, 789.

(80) Goldman, A. *Structure* **1995**, *3*, 1277.

(81) Rice, D. W.; Yip, K. S. P.; Stillman, T. J.; Britton, K. L.; Fuentes, A.; Connerton, I.; Pasquo, A.; Scandurra, R.; Engel, P. C. *FEMS Microbiol. Rev.* **1996**, *18*, 105.

(82) Russell, R. J. M.; Ferguson, J. M. C.; Hough, D. W.; Danson, M. J.; Taylor, G. L. *Biochemistry* **1997**, *36*, 9983.

structure of the enzyme was modified upon immobilization on clays, adopting a catalytically active conformation with a lower α -helix content.

Biochemical characterization of immobilized β -glucosidase revealed that the microenvironment created by the aluminosilicate materials under investigation induced beneficial changes for the catalytic behavior of the enzyme. The improved pH and temperature profiles that were observed for hybrid biocatalysts could enlarge the potential of β -glucosidase for industrial-scale applications.⁴⁴ In addition, the multicharged clay matrix can affect the affinity of enzyme toward the substrate, and most interestingly, favor interactions that stabilize the enzyme against thermal denaturation. The present results indicate that these smectite nanoclays

are promising materials that can be used as matrices for the immobilization of enzymes. The use of these clays for the immobilization of various enzymes such as hydrolases and oxidoreductases is under investigation.

Acknowledgment. This work received financial support from the Dutch Foundation for Fundamental Research on Matter (FOM) and the Breedtestrategie program of the University of Groningen as well as from the Greek General Secretariat of Research and Technology, within the framework of the PENED (03-ED167) research program. I.V.P. was financially supported by the Bodossakis Foundation. The authors gratefully acknowledge the use of the XRD unit of the Laboratory Network, UOI.

CM800486U